

# Peak-temperature patterns of polyphase metamorphism resulting from accretion, subduction and collision (eastern Tauern Window, European Alps) – a study with Raman microspectroscopy on carbonaceous material (RSCM)

A. SCHARF,<sup>1</sup> M. R. HANDY,<sup>1</sup> M. A. ZIEMANN<sup>2</sup> AND S. M. SCHMID<sup>1,3</sup>

<sup>1</sup>Department of Earth Sciences, Freie Universität Berlin, Malteserstrasse 74-100, Berlin, 12249, Germany (andreas.scharf@fu-berlin.de)

<sup>2</sup>Institute of Earth and Environmental Science, Universität Potsdam, Karl-Liebknecht-Strasse 24-25, Potsdam-Golm, 14476, Germany

<sup>3</sup>Now at: Department of Geophysics, Eidgenössische Technische Hochschule (ETH), Sonneggstrasse 5, Zürich, 8092, Switzerland

**ABSTRACT** Raman microspectroscopy on carbonaceous material (RSCM) from the eastern Tauern Window indicates contrasting peak-temperature patterns in three different fabric domains, each of which underwent a poly-metamorphic orogenic evolution: Domain 1 in the northeastern Tauern Window preserves oceanic units (Glockner Nappe System, Matrei Zone) that attained peak temperatures ( $T_p$ ) of 350–480 °C following Late Cretaceous to Palaeogene nappe stacking in an accretionary wedge. Domain 2 in the central Tauern Window experienced  $T_p$  of 500–535 °C that was attained either within an exhumed Palaeogene subduction channel or during Oligocene Barrovian-type thermal overprinting within the Alpine collisional orogen. Domain 3 in the Eastern Tauern Subdome has a peak-temperature pattern that resulted from Eo-Oligocene nappe stacking of continental units derived from the distal European margin. This pattern acquired its presently concentric pattern in Miocene time due to post-nappe doming and extensional shearing along the Katschberg Shear Zone System (KSZS).  $T_p$  values in the largest (Hochalm) dome range from 612 °C in its core to 440 °C at its rim. The maximum peak-temperature gradient ( $\leq 70$  °C km<sup>-1</sup>) occurs along the eastern margin of this dome where mylonitic shearing of the Katschberg Normal Fault (KNF) significantly thinned the Subpenninic- and Penninic nappe pile, including the pre-existing peak-temperature gradient.

**Key words:** doming; Eastern Alps; high-pressure and Barrovian-type metamorphism; orogen-parallel extension; peak-temperature pattern; Raman microspectroscopy.

**Abbreviations:** CI, confidence interval; CM, carbonaceous material; ETD, Eastern Tauern Subdome; KNF, Katschberg Normal Fault; KSZS, Katschberg Shear Zone System;  $T_p$ , peak temperature; RSCM, Raman microspectroscopy on carbonaceous material; SEMP, Fault Salzach-Ennstal-Mariazell-Puchberg Fault; WTD, Western Tauern Subdome.

## INTRODUCTION

The Tauern Window in the Eastern Alps exposes a nappe pile of continental and oceanic units (Subpenninic- and Penninic units respectively) that underwent Cenozoic subduction, collision, and metamorphism during convergence of the Adriatic and European plates (e.g. Trümpy, 1960; Frisch, 1979; Tricart, 1984; Haas *et al.*, 1995; Stampfli *et al.*, 2001; Schmid *et al.*, 2004). The structurally deepest nappes of these units experienced upper amphibolite facies metamorphism centred on two domes at either end of the Tauern Window (e.g. Selverstone *et al.*, 1984; Cliff *et al.*, 1985; Oberhänsli *et al.*, 2004), namely, the Eastern and Western Tauern subdomes (ETD and

WTD in Fig. 1). In contrast, the centre of the window preserves structurally higher nappes that were less affected by Barrovian-type thermal overprint and, hence, contain relicts of earlier high-pressure metamorphism, including blueschist and eclogite facies mineral assemblages (e.g. Dachs, 1986; Dachs & Proyer, 2001). <sup>40</sup>Ar/<sup>39</sup>Ar dating of phengite from these assemblages (Zimmermann *et al.*, 1994; Ratschbacher *et al.*, 2004; Kurz *et al.*, 2008) combined with geodynamic arguments (see discussion in Schmid *et al.*, 2013) suggests that this high-pressure metamorphism occurred in Middle Eocene time, prior to the attainment of peak temperatures ( $T_p$ ) in the domes during the Oligocene (Kurz *et al.*, 2008). Previous work on the distribution and conditions of

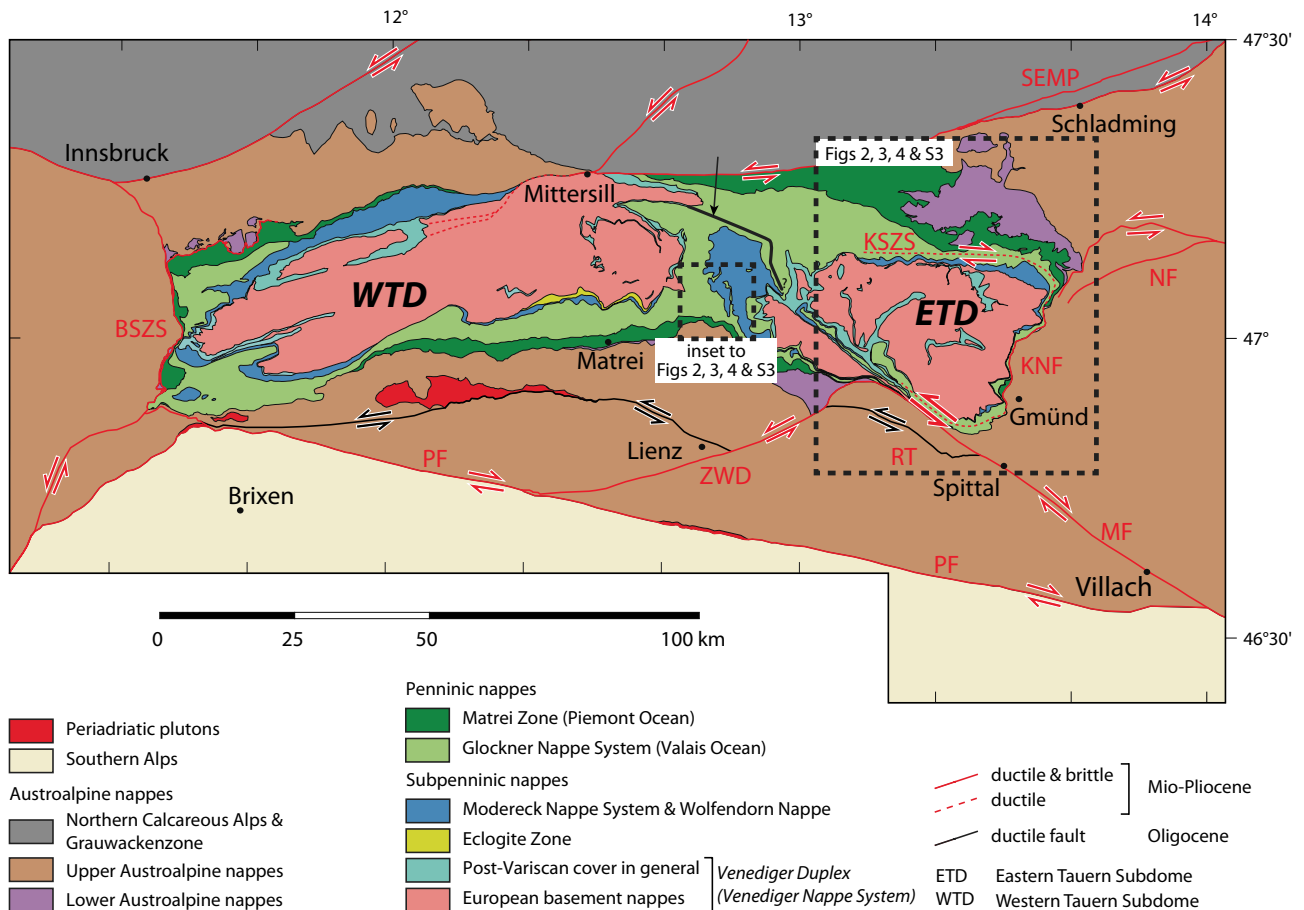


**Fig. 1.** Tectonic map of the Tauern Window modified from Schmid *et al.* (2013). Dotted frames indicate the investigated areas. BSZS, Brenner Shear Zone System; KNF, Katschberg Normal Fault; KSZS, Katschberg Shear Zone System; MF, Mölltal Fault; NF, Niedere Tauern Southern Fault; PF, Periadriatic Fault; RT, Ragga-Teuchl Fault; SEMP, Salzach-Ennstal-Mariazell-Puchberg Fault; ZWD, Zwischenbergen-Wöllatratten-Drau Fault. Arrow marks a thrust in the northern part of the central Tauern Window that separates the southern part of the Glockner Nappe System with high-pressure metamorphic relics from the northern part that was unaffected by high-pressure metamorphism.

regional metamorphism based on equilibrium mineral assemblages (Cliff *et al.*, 1985; Droop, 1985; review in Hoinkes *et al.*, 1999) and stable oxygen isotopes (Droop, 1985) reveals an asymmetrical concentric pattern of peak-temperature isotherms that cut across the nappe contacts in map view (Fig. 2a). This asymmetrical pattern coincides broadly with the ETD containing the structurally lowest basement nappes in its core. This dome is delimited to the east by the Katschberg Shear Zone System (KSZS, Scharf *et al.*, 2013), which comprises an east- to southeast dipping, low-angle extensional shear zone, the Katschberg Normal Fault (KNF, Genser & Neubauer, 1989) and two kinematically connected strike-slip shear zones in the north and south (Figs 1–4 & S3).

Structural studies reveal the KSZS to be a mylonitic belt of up to 5 km width that affects the entire eastern part of the dome, including parts of its deepest unit (Scharf *et al.*, 2013). This raises the possibility that the metamorphic zonation and related  $T_p$  distribution were modified by mylonitic deformation

during extensional exhumation of the Subpenninic- and Penninic units along the KSZS. Furthermore, the preservation of high-pressure assemblages in parts of the Glockner Nappe System of the central part of the Tauern Window (Dachs & Proyer, 2001; Kurz *et al.*, 2008) suggests that the  $T_p$  pattern may be a composite of the overlapping high-pressure and high-temperature metamorphic events.

To test these ideas, Raman microspectroscopy of carbonaceous material (RSCM) from metapelites was applied to obtain the distribution of  $T_p$  in two crucial areas: (i) the transition from the ETD across various segments of the KSZS to the Austroalpine units in the hangingwall of the KSZS (Figs 1–4 & S3); and (ii) the central part of the Tauern Window affected by high-pressure metamorphism (inset in Figs 1–4 & S3). Combining RSCM with thorough structural and petrological analyses proved to be successful in distinguishing Eocene high-pressure metamorphism from the later Barrovian-type thermal overprint. The  $T_p$  values obtained from RSCM – a large number (200)

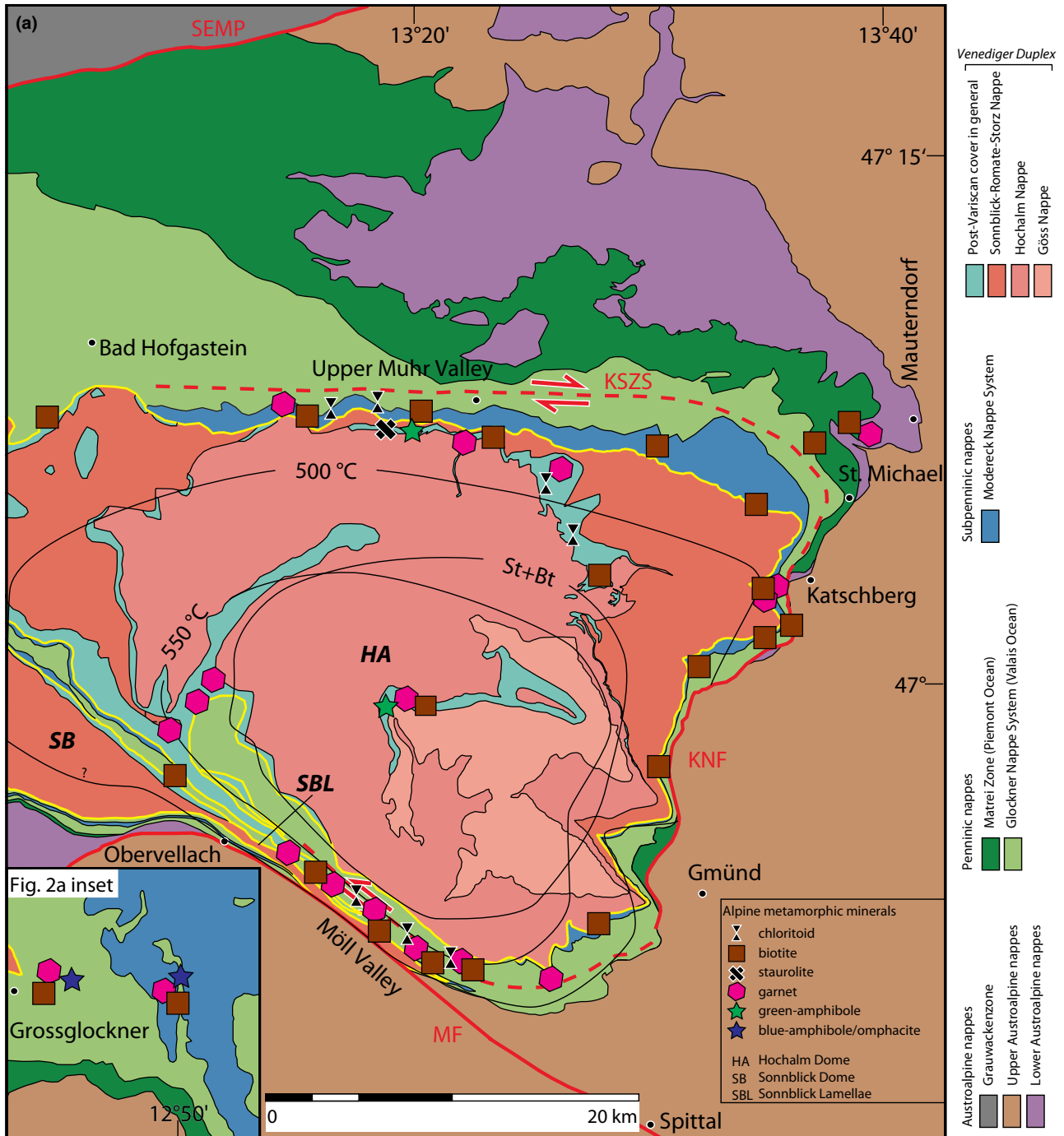


**Fig. 2a.** Tectonic maps of the boxed areas in Fig. 1 for the eastern Tauern Window: (a) main tectonic units including post-nappe folds, peak-metamorphic isotherms and the staurolite + biotite (St + Bt) isograd. Capitalized abbreviations mark the culmination points of the main post-nappe domes. Isotherms taken from Hoinkes *et al.* (1999) except for the 500 °C isotherm in the Sonnblick Dome drawn from our own data. Roof thrust of the Venediger Duplex is marked in yellow.

of samples over a small area ( $50 \times 30 \text{ km}^2$ ) – agree with  $T_p$  estimated from the distribution of peak-metamorphic mineral assemblages. The combination of RSCM with a structural and petrological study of the investigated area (Scharf *et al.*, 2013) allows the  $T_p$  estimates to be set in a geodynamic context.

## PROVENANCE OF THE SAMPLES

### Lithologies

The metasedimentary rocks used in this study (Fig. 3) experienced varied  $P$ – $T$  conditions at different times

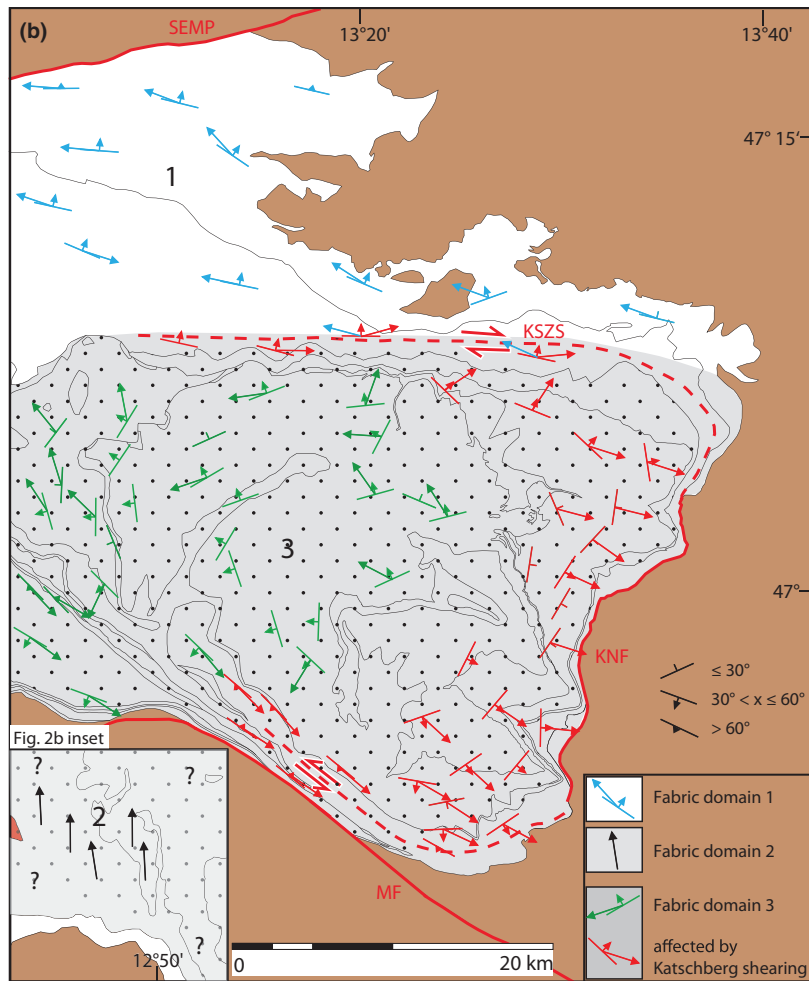


**Fig. 2b.** Tectonic maps of the boxed areas in Fig. 1 for the eastern Tauern Window: (b) Map of fabric domains 1–3 described in text. Orientations of the main mylonitic foliation and stretching lineation taken from Scharf *et al.* (2013). Dotted part of fabric domain 3 is where peak temperatures are clearly associated with the Barrovian-type metamorphism (Tauernkristallisation). Question marks in ‘domain 2’ indicating where the age of the peak temperature is not known (Paleogene subduction and exhumation or Oligocene ‘Tauernkristallisation?’).

during their metamorphic evolution. Fourteen of the samples are from the Austroalpine units, and most of these are from the Katschberg Quartzphyllite of presumed Silurian age (Schönlaub *et al.*, 1976), and from retrogressed pre-Variscan micaschists containing quartz and white mica (Table S1). This group of rocks experienced metamorphism and nappe stacking during the Late Cretaceous Eo-Alpine orogeny (Schuster *et al.*, 2006; Pestal *et al.*, 2009), which affected the northern margin of the Adriatic microplate before the Cenozoic subduction of Alpine Tethys (Handy *et al.*, 2010). One sample (sample 98 in Fig. 3 and Table S1) in the southeastern part of the area comes from an Austroalpine unit that experienced Late Cretaceous eclogite facies metamorphism (Thöni, 2006), but the sample itself contains only an amphibolite facies mineral assemblage (Table S1). Eo-Alpine orogenesis is not the subject of this study, but the samples were included because they yield information about  $T_p$  in the hangingwall of the KSZS.

Most samples are calc-schists and black shales of the so-called ‘Bündnerschiefer’ of the Glockner

Nappe System (116 samples) and the Matreier Zone (33 samples) that derived from Alpine Tethys (Figs 1–3). The term ‘Bündnerschiefer’ is used as a field term for schist containing white mica, chlorite, quartz and calcite that is sometimes associated with lenses of prasinite (greenschist facies epidote-chlorite-albite-bearing metabasic rock), as well as rare pods of serpentinite. This association is interpreted to be diagnostic of oceanic lithosphere or of lithosphere formed at the ocean–continent transition of Alpine Tethys (e.g. Lemoine *et al.*, 1987). Alpine Tethys was actually a composite of two oceans: the Piemont-Liguria Ocean that opened in Early–Middle Jurassic times (Matreier Zone) and the Valais Ocean that opened in Late Jurassic to Early Cretaceous times (Glockner Nappe System). Calc-schist of the Matreier Zone typically contains pelagic metasedimentary rocks (e.g. radiolarite) and blocks of Austroalpine rock derived from the formerly adjacent Adriatic margin, whereas the ‘Bündnerschiefer’ of the Glockner Nappe System lacks these elements and generally contains fewer ultramafic bodies (see reviews in Pestal *et al.*, 2009; Schmid *et al.*, 2013).

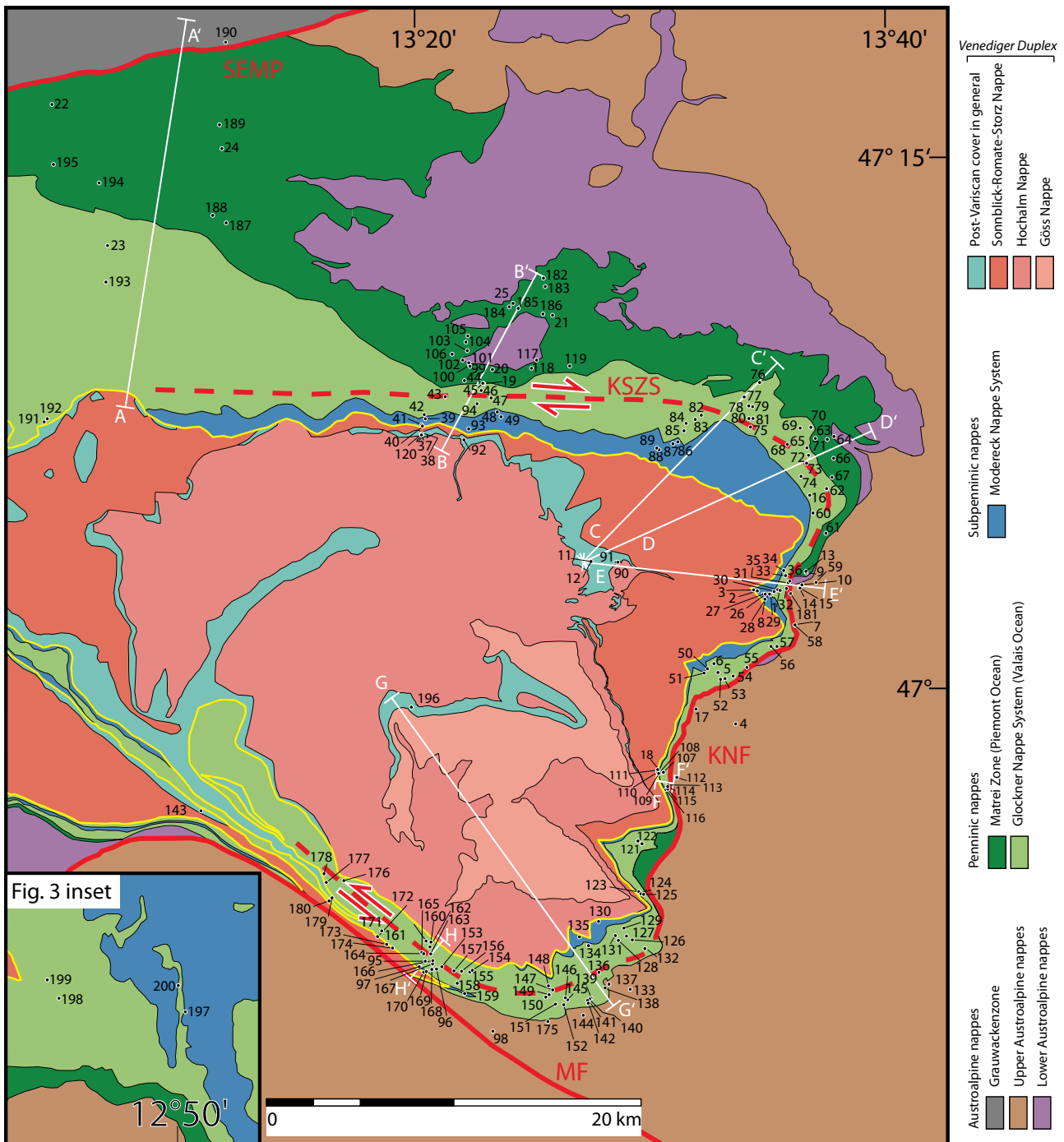


**Fig. 3.** Tectonic map of the eastern part of the Tauern Window and of the Grossglockner area (inset). Numbers refer to samples and their locations (Table S1). White lines show traces of cross-sections a–h in Fig. 5. Roof thrust of the Venediger Duplex is marked in yellow. Area of map is indicated by box in Fig. 1.

In the central part of the Tauern Window, i.e. near the highest Austrian mountain, the Grossglockner (3798 m), the Glockner Nappe System can be subdivided into two parts (Frasl & Frank, 1966) separated by a major thrust (black arrow in Fig. 1, taken from Pestal & Hejl, 2005): a southern part that preserves

eclogite- and blueschist facies mineral assemblages (e.g. Dachs & Proyer, 2001; Kurz *et al.*, 2008) of Eocene age (e.g. Kurz *et al.*, 2008), and a northern part with greenschist facies assemblages and no evidence of high-pressure metamorphism (e.g. Hejl, 1984; Slapansky & Frank, 1987; Liu *et al.*, 2001;

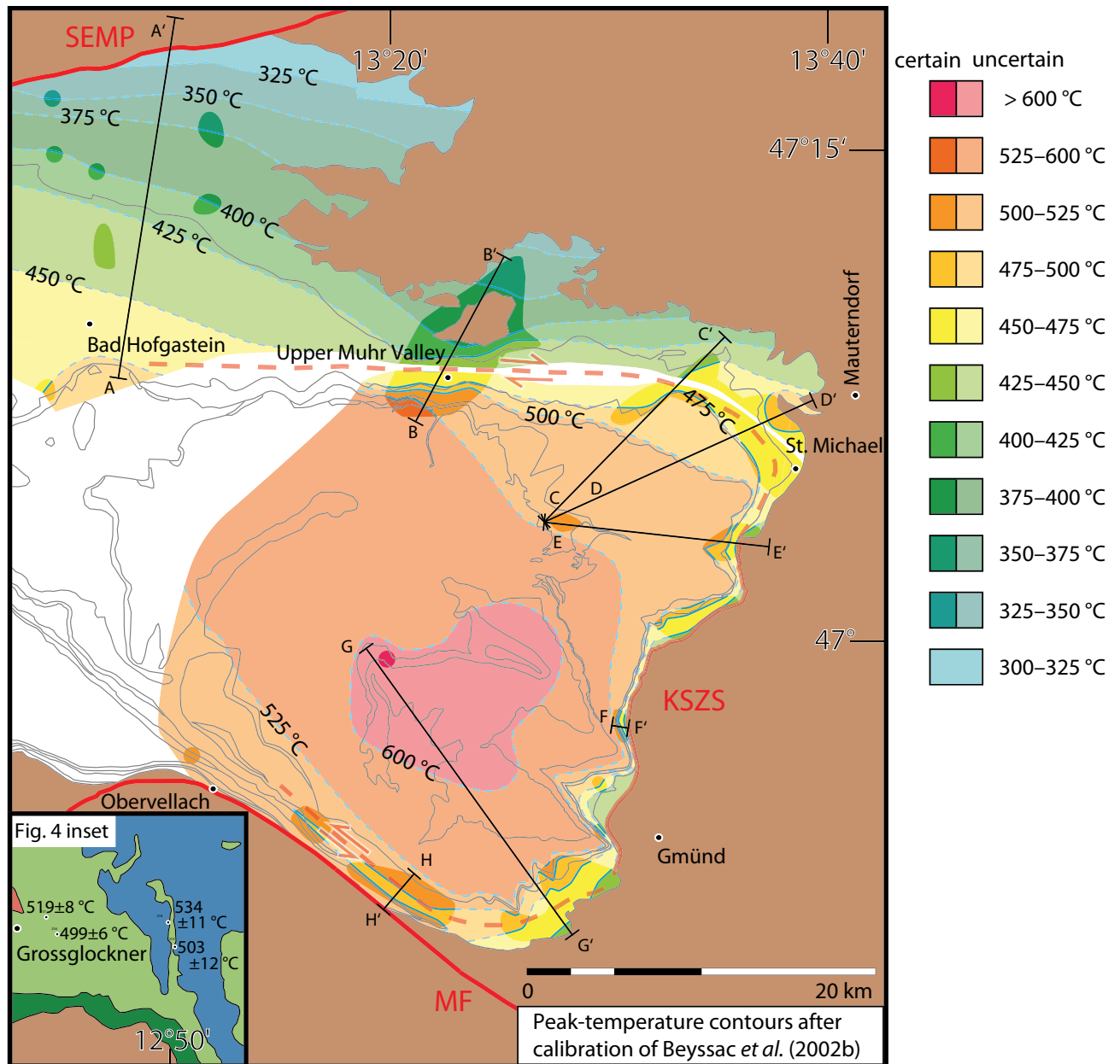


**Fig. 4.** Peak-temperature contours in fabric domains 1 and 3 are based on the calibration of Beyssac *et al.* (2002b). Transparent colours and dashed lines indicate areas and contours where the sample density is low. Brown colours indicate Austroalpine units. Grey lines indicate tectonic contacts separating units of the Tauern Window as shown in Figs 2a & 3. The peak-temperature contours are marked in blue. KSZS, Katschberg Shear Zone System; MF, Mölltal Fault; SEMP, Salzach-Ennstal-Mariazell-Puchberg Fault. Inset shows peak temperatures from four samples in fabric domain 2. No peak-temperature contours appear in the inset area due to the limited number of samples and their similar peak-temperature values. Therefore, the tectonic units as in Figs 2a & 3 are shown in the inset. Note that the broader peak-temperature interval (75 °C rather than the usual 25 °C) in the core of the ETD reflects the limited number of samples (three). Sample locations and data shown in Fig. 3 and Table S1.

Pestal *et al.*, 2009; Pestal & Hellerschmidt-Alber, 2011), the so-called Glockner- and Fuscher Facies respectively (Pestal *et al.*, 2009). Four samples come from the Glockner Facies (inset in Figs 3 & 4 & S3 and Table S1), which experienced peak-metamorphic conditions of 570 °C/1.7 GPa (Dachs & Proyer,

2001; Kurz *et al.*, 2008). Calc-schist in this unit contains lawsonite and/or albite + epidote + phengite + chlorite as pseudomorphs after lawsonite (Gleissner *et al.*, 2007).

A third group of 36 samples was collected in Subpenninic units comprising basement and cover

derived from the former European continental margin. Nine of these samples come from the post-Variscan cover of three tectonic basement slices (Göss-, Hochalm- and Sonnblick-Romate-Storz nappes; Figs 2a & 3) that make up a duplex structure in the core of the ETD (Venediger Duplex of Schmid *et al.*, 2013). These units all experienced upper greenschist to amphibolite facies, Barrovian-type metamorphism ('Tauernkristallisation' of Sander, 1911) at peak conditions of 630 °C and 0.8 GPa (Göss Nappe; Droop, 1985) at *c.* 30–28 Ma (Rb/Sr white mica ages; Inger & Cliff, 1994; Thöni, 1999; Kurz *et al.*, 2008). The basement is variegated, with pre-Variscan metasedimentary rocks and Late Palaeozoic granitoid intrusive rocks overlain by a Late Palaeozoic to Mesozoic cover, which experienced only Cenozoic Alpine metamorphism (Pestal *et al.*, 2009). These cover rocks are mostly carbonates (Silbereck Serie of Exner, 1939), meta-pelites containing white mica and quartz, and meta-arkoses. One sample of white mica-garnet schist was taken from the cover of the Göss Nappe, the structurally lowest basement unit of the Venediger Duplex (Fig. 3, light blue domain between Göss- and Hochalm basement units; sample 196 in Fig. 3 and Table S1). The protolith age of this cover (quartz-rich rocks intercalated with biotite-bearing metasedimentary rocks and meta-volcanites; the so-called Draxel Complex of Exner, 1971, 1980) is controversial with ages proposed ranging from Latest Devonian (Kebede *et al.*, 2003; Lerchbauer, 2008), Early Carboniferous (Pestal *et al.*, 2009) and Late Carboniferous-Permian (Schmid *et al.*, 2013). These rocks are clearly Late Palaeozoic in age ('Jungpaläozoikum' of Schuster *et al.*, 2006) and a post-Variscan age of sedimentation is likely based on well-documented evidence for coeval sedimentation and magmatic activity in the Late Carboniferous to Permian time in other parts of the Tauern Window (Veselà *et al.*, 2008, 2011). Thus, the metamorphism of the rocks of the Draxel Complex is interpreted to be of Alpine age (Schmid *et al.*, 2013).

The remaining 27 of the 36 Subpenninic samples were collected from the structurally highest Subpenninic unit, the Modereck Nappe System (e.g. Kurz *et al.*, 2008; Schmid *et al.*, 2013), which is in-folded with a part of the Glockner Nappe System to form the so-called Seidlwinkl Fold, exposed in the Grossglockner area above the roof thrust of the Venediger Duplex (Figs 2a & 3). The units of the Modereck Nappe System originate from the most distal part of the European margin (Kurz *et al.*, 2008; Schmid *et al.*, 2013). Their cover rocks contain mostly siliciclastic metapelite with albite, biotite and chlorite, although some horizons contain evaporite and black shale. The age of these rocks ranges from Late Permian to Late Cretaceous (e.g. Pestal *et al.*, 2009; Schmid *et al.*, 2013), which constrains the metamorphic overprint of these rocks to be Alpine in age.

### Fabric domains in the sampling area

The eastern part of the Tauern Window is divided into three fabric domains based on the orientation and relative age of structures, as well as on the mineral parageneses associated with the main foliation (Fig. 2a,b; Scharf *et al.*, 2013):

**Domain 1:** A greenschist facies domain between the Salzach-Ennstal-Mariazell-Puchberg (SEMP) Fault (Ratschbacher *et al.*, 1991) in the north and the northern branch of the KSZS in the south (Scharf *et al.*, 2013) is characterized by a WNW-ESE striking main foliation (blue symbols in Fig. 2b). This foliation is deformed by and therefore predates the SEMP and KSZS fault structures. This older fabric deforms the base of the Lower Austroalpine nappes, which are only affected by sub-greenschist facies Alpine metamorphism (e.g. Becker, 1993; Oberhänsli *et al.*, 2004 and references therein; Schuster *et al.*, 2004).

**Domain 2:** This is a blueschist-to eclogite facies domain in which the main foliation carries a subhorizontal north-south trending stretching lineation associated with top-north sense of shear (black stretching lineations in Fig. 2b). This foliation is deformed by, and therefore older than, large post-nappe folds making up the ETD (e.g. Sonnblick- and Hochalm domes in Fig. 2a; D5 of Schmid *et al.*, 2013). The boundary between domains 1 and 2 is a thrust (see above and Fig. 1, Pestal & Hejl, 2005) that emplaced the part of the Glockner Nappe System containing high-pressure mineral assemblages onto the northern part of the Glockner Nappe System that lacks evidence of subduction metamorphism.

**Domain 3:** This is a greenschist- to amphibolite facies domain in the vicinity of the ETD and the KSZS (Scharf *et al.*, 2013). Rocks in this domain have two main foliations: an older schistosity (green symbols in Fig. 2b) that is overgrown by prograde high-temperature mineral assemblages of the so-called 'Tauernkristallisation', deformed by the aforementioned domes, and a younger mylonitic foliation (red symbols in Fig. 2b) affecting the perimeter of the ETD under retrograde upper greenschist facies conditions and associated with the KSZS. This shear zone system accommodated east- to southeast-directed orogen-parallel motion, including top-southeast exhumation of the Subpenninic- and Penninic units in the footwall of the aforementioned KNF. The northern and southern branches of the KSZS are steeply dipping strike-slip shear zones that are interpreted as stretching faults, with decreasing amounts of displacement towards their western ends (Scharf *et al.*, 2013).

### Sampling strategy

Most samples were collected within domain 3, which includes the Subpenninic-, Penninic- and Austroalpine nappes in the hangingwall of the KSZS. The coverage of domains 1 and 2 was more limited, but

still sufficient to allow an interpretation of the geodynamic significance of pre-collisional thermal events. Samples were taken as far north as the SEMP Fault along the northern limit of the Tauern Window. One sample (sample 190 in Fig. 3 and Table S1) was collected north of this fault in an Upper Austroalpine unit.

## RAMAN MICROSPECTROSCOPY ON CARBONACEOUS MATERIAL

### The method

Carbonaceous material (CM) transforms from poorly ordered, highly contaminated matter (e.g. H, N, O, S of the original organic compounds) to well-ordered graphite with increasing temperature. The ordering of carbon atoms, known as graphitization (Teichmüller, 1987), is highly temperature-dependent and does not re-equilibrate or restructure with decreasing temperature during retrograde metamorphism. Therefore, graphitization is an irreversible process and the degree of carbon ordering in a natural rock can be used as an indicator of peak-metamorphic temperature (e.g. Quinn & Glass, 1958; French, 1964; Landis, 1971; Grew, 1974; Itaya, 1981; Buseck & Bo-Jun, 1985).

The Raman spectra of CM in a sample primarily reflect the degree of ordering of carbon atoms attained at  $T_p$  (e.g. Pasteris & Wopenka, 1991; Wopenka & Pasteris, 1993). Several temperature calibrations based on the degree of ordering are currently available (Beysac *et al.*, 2002b; Rahl *et al.*, 2005; Aoya *et al.*, 2010). For a reliable interpretation of the RSCM results, some basic considerations need to be taken into account to make the results of the RSCM method more robust and reliable:

- (1) Ideally one single and distinct thermal peak is assumed to yield a characteristic distribution of  $T_p$  values. To unravel  $T_p$  distributions associated with multiple metamorphic events, a suite of samples needs to be collected over a sufficiently large area (in our study some  $50 \times 30 \text{ km}^2$ ) to ensure that only one event predominated within a given part of the total area covered. In our study, earlier high-pressure metamorphism in the Glockner Nappe System was overprinted by a later Barrovian-type metamorphic event, a setting that is similar to that analysed with RSCM in the Central Alps (Wiederkehr *et al.*, 2011).
- (2) Beysac *et al.* (2002a, 2003a) showed that pressure effects on ordering of CM can be neglected. However, other factors that need to be taken into account when interpreting CM spectra include the duration of the thermal event (Itaya, 1981; Okuyama-Kusunose & Itaya, 1987; Aoya *et al.*, 2010), differential stress (Bustin *et al.*, 1986; Suchy *et al.*, 1997; Ferreira Mählmann *et al.*, 2002; Nover *et al.*, 2005), host rock composition (Grew, 1974;

Wopenka & Pasteris, 1993; Wada *et al.*, 1994), occurrence of catalytic minerals (Bonijoly *et al.*, 1982; Okuyama-Kusunose & Itaya, 1987 and references therein), type of organic precursor (Kribek *et al.*, 1994; Large *et al.*, 1994; Bustin *et al.*, 1995) and the composition and activity of fluids (Large *et al.*, 1994; Guedes *et al.*, 2005). These factors are discussed below when dealing with observed multi-temperature signal in the same sample, but most previous studies indicate that these effects are minor compared with that of temperature (e.g. Beysac *et al.*, 2002b; Rahl *et al.*, 2005; Aoya *et al.*, 2010; Lahfid *et al.*, 2010; Wiederkehr *et al.*, 2011).

The RSCM method offers several advantages when compared with other analytical methods in metamorphic rocks, which are also based on CM (X-ray diffraction, high-resolution transmission electron microscopy (HRTEM), isotope geochemistry and vitrinite reflectance measurement): first, sample preparation is straightforward and requires only a standard polished (for microprobe) thin section, which can be used for different types of investigations. Raman spectra can be acquired quickly (within few minutes per analysis) and several spots can be analysed in a single sample, allowing heterogeneities to be identified. Second, the method is in situ and does not destroy the sample. Third, the amount of CM required for an analysis is very small; 20–30 grains of 10  $\mu\text{m}$  diameter are the minimum amount and size of material needed. Fourth, the range of  $T_p$  can be estimated over a very large range of metamorphic conditions, from sub-greenschist to upper amphibolite facies. The RSCM calibrations are all based on temperatures obtained by other analytical methods (e.g. Fe-Mg exchange reactions); hence, the absolute error of the RSCM method ( $\pm 50 \text{ }^\circ\text{C}$ ; Beysac *et al.*, 2002b) can be attributed mostly to the absolute error of these methods. However, the error of relative temperature estimates is significantly smaller ( $\sim \pm 10\text{--}15 \text{ }^\circ\text{C}$ , Beysac *et al.*, 2004) than the error of absolute peak-temperature estimates. Note that the distribution of  $T_p$  values within a study is equally important for enabling certain interpretations as are the absolute values of  $T_p$ ; the distribution pattern in map view can be diagnostic for deciphering the tectonometamorphic history.

### Measurement procedure

This study employed the method of Wiederkehr *et al.* (2011) at a laser wavelength of 532 nm, which is shifted slightly to the 514.5 nm laser line used in the calibration experiments of Beysac *et al.* (2002b), but nevertheless yields a difference in the estimate of  $T_p$  of only 5  $^\circ\text{C}$  or less (Aoya *et al.*, 2010). This is much less than the errors cited above in estimating the absolute and relative values of  $T_p$ .

Care was taken to measure CM located beneath a transparent mineral (quartz, albite or white mica) at the sample surface (Pasteris, 1989; Beyssac *et al.*, 2002b, 2003b). The effect of analysing through two different transparent minerals was checked (white mica and albite in sample 2; Fig. 3 and Table S1). In doing so, it was found that the  $T_p$  values were identical within error (confidence interval, [CI] of 95%; see caption to Table S1 for further explanation). Where possible, the polarized laser beam was oriented perpendicular to the local mean stacking axis of the CM. Any spectra with bands from the glue (used for thin section preparation, Araldit AV 2020; refraction index of 1.553) overlying the graphite spectra were not used at all.

In almost every sample, 20 single spots of CM were measured (column #spec. R1 of Table S1). Each measurement was conducted 10 times, with a pulse duration of 12 s per measurement. Thus, the full acquisition time was 120 s per aggregate of CM in a sample. Aberrant estimates of  $T_p$  (i.e. estimate that deviated by >50 °C from the average) were ignored in making the overall estimate, as long as their number did not exceed six of the 20 estimates from spot analyses. Usually, however, no more than three estimates were aberrant. The exact number of aberrant spots in a given sample equals to the discrepancy of the number of recorded Raman spectra (#spec. R1) and the number of Raman spectra used for peak-temperature calculation (#spec. R1\*) in Table S1. Samples with <10 single spot analyses are listed in Table S1, but were not used for drawing the peak-temperature contours in Figs 4 and S3. The position, height and width of the CM peaks (FWHM, full width at half maximum) of the single Raman spectra were determined with the program PEAKFIT 4.12 (Seasolve Software Inc.). This program identifies the peaks with a combined Gaussian and Lorentzian function (Voigt function) including a linear background correction. Error is estimated for a CI of 95%.

### Peak-temperature calibrations

Table 1 lists the four empirical temperature calibrations of the Raman spectra for CMs used in this study. They are applicable for a temperature range of 100–700 °C and use the intensity ratios, R1 and R2,

**Table 1.** Raman peak-temperature calibrations from literature and specifications as used in this study.

	Calibration $T(^{\circ}\text{C})=$	Peak-temperature range ( $^{\circ}\text{C}$ )	Laser wavelength (nm)	Reference
a	$-445\text{R2} + 641$	350–650	514.5	Beyssac <i>et al.</i> (2002b)
b	$737.3 + 320.9\text{R1} - 1067\text{R2} - 80.638\text{R12}$	100–700	532	Rahl <i>et al.</i> (2005)
c	$221\text{R22} - 637.1\text{R2} + 672.3$	340–655	514.5	Aoya <i>et al.</i> (2010)
d	$91.4\text{R22} - 556.3\text{R2} + 676.3$	340–655	532	Aoya <i>et al.</i> (2010)

of the first-order Raman peaks D1–D3 and G. Further details of the calibrations are given in Appendix S1. These ratios are defined as  $\text{R1} = \text{D1}/\text{G}$  (height of the peaks) and  $\text{R2} = \text{D1}/(\text{G} + \text{D1} + \text{D2} + \text{D3})$  (area beneath the peaks) and are a measure of the degree of ordering of CM as a function of maximum temperature (Pasteris & Wopenka, 1991; Wopenka & Pasteris, 1993; Yui *et al.*, 1996). Second-order bands of the Raman spectra were not used in this study because their relationship with the degree of carbon ordering is less clear (e.g. Nemanich & Solin, 1979; Beyssac *et al.*, 2002b).

Although the calibrations of Beyssac *et al.* (2002b) and Aoya *et al.* (2010, calibration d in Table 1) yield similar values and are in best agreement with the petrology (see Discussion section). The Beyssac *et al.* (2002b) calibration is used instead of the calibration of Aoya *et al.* (2010, calibration d in Table 1) because its formula is simpler than the others and therefore yields a consistently lower CI (see Table S1), even at  $T_p$  above 575 °C where the error tends to be greater. Comparisons and discussion relevant to the Raman calibrations used in this study are given in Appendix S1 (Figs S1–S3 & Table S1).

## RESULTS

### Contouring peak temperatures

The map view contours of  $T_p$  (Fig. 4) based on the calibration of Beyssac *et al.* (2002b) were hand drawn to interpolate between bracketing points of the  $T_p$ , and to follow the main foliation in the fabric domains described above. Hand drawing allows fitting contours with the main foliation and avoids edge effects where sample density is small and/or where points of anomalous  $T_p$  occur, i.e.  $T_p$  values that obviously do not fit the overall pattern (see below). Contours of  $T_p$  obtained from other calibrations (Table 1) are shown in Fig. S3 for comparison. Note that contours of  $T_p$  are not isotherms. An isotherm is a line of equal temperature at a given instant in time, whereas contours of  $T_p$  contain no information about the time when  $T_p$  was reached. A pattern of  $T_p$  contours, referred to as peak-temperature contours (identical with the 'isotemperature contours' of Wiederkehr *et al.*, 2011) can only be interpreted as representing a palaeotemperature field if the area considered was affected by a single thermal event. Even in such a simple case, peak-temperature contours are expected to decrease in age away from the heat source as the temperature field expanded until the area considered reached its thermal peak. Of course, the interpretation in terms of age becomes even more difficult in areas, such as ours, affected by two or more thermal events with comparable  $T_p$  conditions. Hence, the peak-temperature contours in Fig. 4 merely represent  $T_p$  attained in the three fabric domains described above and depicted in Fig. 2b. Uncoloured strips separate the

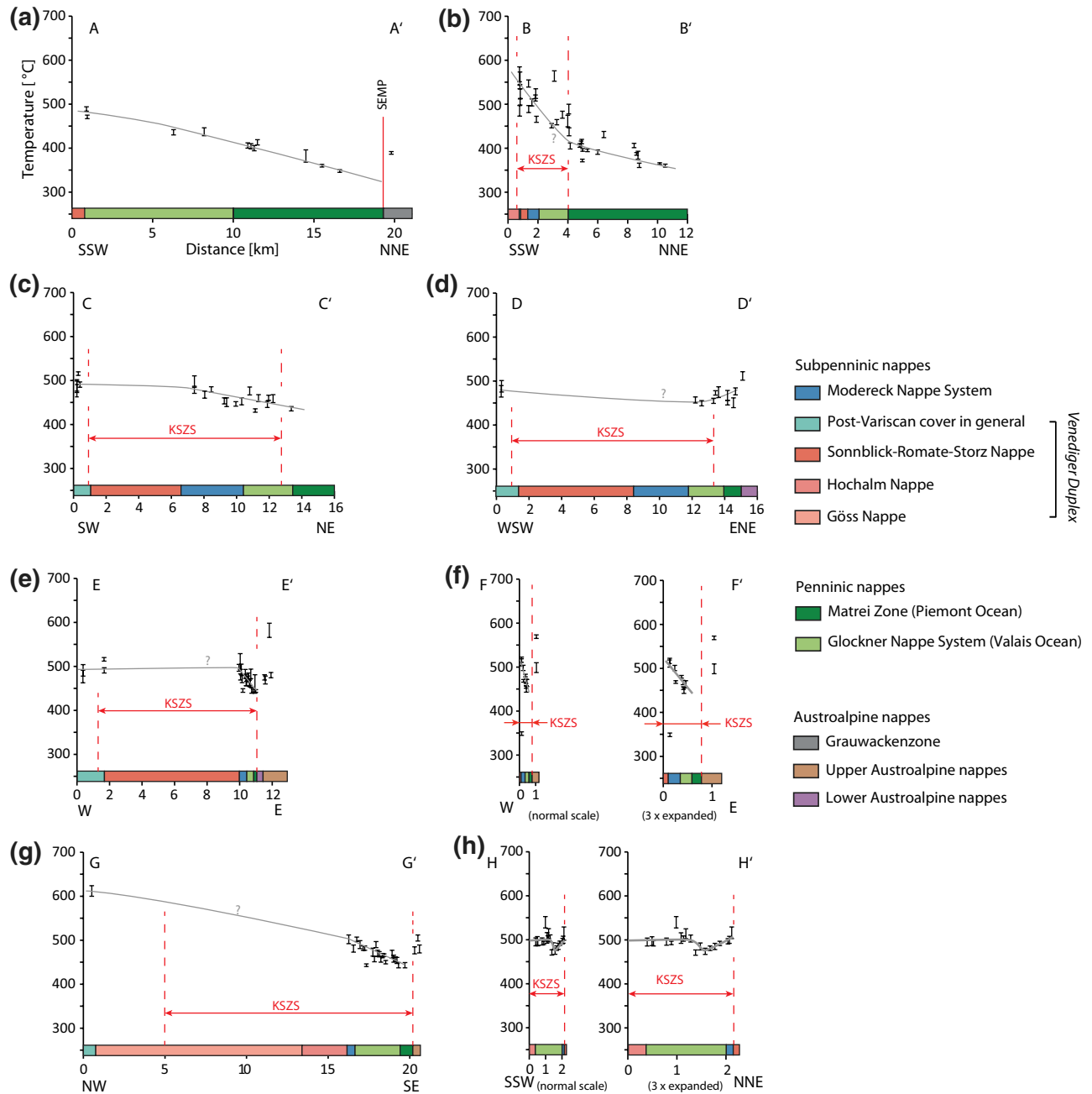


**Fig. 5.** Cross-sections (a–h) of peak temperature along traces shown in Fig. 4. Calibration of Beyssac *et al.* (2002b) with individual CI (95%) bars. Colours along the horizontal axes indicate the tectonic units in Figs 1, 2a, 3, 4 & S3. Red dotted lines indicate boundaries of the Katschberg Shear Zone System (KSZS) in cross-sections b–h. Note that the horizontal axes in the additional drawings in sections f and h are expanded by a factor of 3 for easier viewing. Peak-temperature points are projected parallel to the main foliation into the sections from as far as 2.5 km on either side of the section planes, except in Fig. 5a where the projection is up to 5 km from the plane.

temperature patterns within these domains. Peak-temperature contours were not drawn for domain 2 (inset to Fig. 4) because the four samples do not warrant contouring, and have almost the same  $T_p$  values. In the following, the pattern of peak-temperature estimates in each of the three fabric domains will be discussed.

**Domain 1**

In the southernmost and structurally lowest part of the Glockner Nappe System north of the KSZS,  $T_p$  decreases systemically from south ( $471 \pm 4$  to  $489 \pm 5$  °C) to north ( $348 \pm 3$  °C), without a discernable discontinuity across the contact between

Glockner Nappe System and Matrei Zone (Fig. 4; and cross-section A-A' Fig. 5a). Trend and spacing of the contours are rather speculative given the paucity of data in this domain; three points define the 400 °C contour, which runs parallel to the trace of the main foliation (Fig. 2b). Accordingly, the other contours are drawn parallel to the main foliation.  $T_p$  values of <350 °C are not found, due to the evident lack of CM in carbonate rocks ('Klammkalke') in this area. However, the  $T_p$  values in this domain probably correspond to lowermost greenschist facies conditions, as previously mapped (Hoinkes *et al.*, 1999; Oberhänsli *et al.*, 2004; Pestal *et al.*, 2009) and estimated with the RSCM method for one sample (Frost *et al.*, 2011). Frost *et al.* (2011) obtained a slightly higher  $T_p$  of ~400 °C in Penninic units at the northeastern margin of the Tauern Window, immediately south of the SEMP Fault. A similar trend of NNE-ward-decreasing  $T_p$  is observed further to the east in the Matrei Zone, i.e. north of the northern branch of the KSZS (Fig. 5b). This corresponds to a peak-temperature field gradient of 8 °C km<sup>-1</sup> perpendicular to the main foliation. One sample (sample 190; Table S1; Fig. 3) within the Grauwackenzone north of the SEMP Fault indicates a higher  $T_p$  (389 ± 3 °C). This higher temperature is attributed to Late Cretaceous greenschist facies (Schramm, 1980) metamorphism (<sup>40</sup>Ar/<sup>39</sup>Ar white mica ages of *c.* 115–90 Ma; Urbanek *et al.*, 2002).

### Domain 2

$T_p$  values of ~500 °C are obtained for the four samples collected within this fabric domain and characterized by blueschist to eclogite facies mineral assemblages (inset to Figs 2a & 4). Similar  $T_p$  values in both the Glockner- and the Modereck nappe systems (green and blue tectonic units in Figs 1–6 & S3) suggest that both units experienced a common thermal history during either Middle to Late Eocene subduction/exhumation, or Oligocene Barrovian-type 'Tauernkristallisation'. In the absence of age data from several independent geochronological systems, the  $T_p$  values in this domain cannot be attributed to one or the other of these two metamorphic events.

### Domain 3

The concentric pattern of peak-temperature contours in this domain mimics the shape of the isograds around the ETD (Fig. 2a). The area with highest  $T_p$  (612 °C, sample 196 in Table S1; Fig. 3) in the Göss Nappe in the core of the ETD coincides with the centre of the concentric foliation pattern (Fig. 2b). However, the contours are poorly constrained due to the lack of CM in the orthogneisses that make up large parts of the dome. The contours are drawn so as to follow the main foliation around the Hochalm Dome.

This is based on our observation that the dome deforms the main foliation, which itself is overgrown by amphibolite facies peak-metamorphic mineral assemblages of the 'Tauernkristallisation' (Scharf *et al.*, 2013). The eastern perimeter of the Hochalm Dome was highly sheared by the KSZS during Miocene time and, hence, the peak-temperature contours are drawn parallel to the main foliation of the KSZS in this part of the Hochalm Dome. Within the ETD, the locally variable trend of the contours (Fig. 4) reflects the heterogeneous orientation of the main foliation.

Going from the core of the ETD towards the KSZS, the horizontal gradient in  $T_p$  varies from ~30 °C km<sup>-1</sup> in the centre (cross-sections B and H, Fig. 5b,h) to as much as 70 °C km<sup>-1</sup> in the immediate footwall of the KNF (cross-sections E and F, Fig. 5e,f) where the post-metamorphic tectonic omission of Penninic and Subpenninic units in the footwall of the KNF is greatest (Scharf *et al.*, 2013). The gradient also increases towards the steep strike-slip branches of the KSZS (cross-section B, Fig. 5b).

A subtle but significant feature in Figs 4 and 5h is a narrow minimum with  $T_p$  values of 475–500 °C located between two stripes characterized by higher  $T_p$  (500–525 °C), located along the southern branch of the KSZS. The southern stripe exhibiting relatively higher  $T_p$  (500–525 °C) coincides with the southeastern end of the Sonnblick Gneiss Lamellae (SBL in Fig. 2a, wedge tapering out southeastward of the Sonnblick Dome, SB), whereas the northern stripe marks the edge of the Hochalm Dome (HA in Fig. 2a). The stripe characterized by lower  $T_p$  (475–500 °C) coincides with the southeastern prolongation of the Mallnitz Synform. Hence, this relative minimum is interpreted as a manifestation of isoclinal folding and Katschberg strike-slip shearing that post-dated both nappe stacking and 'Tauernkristallisation' in the entire ETD (Scharf *et al.*, 2013).

Note that the peak-temperature gradient across the Sonnblick-Romate-Storz Nappe in the northeastern part of the ETD (Fig. 5c,d) appears to be very low to non-existent, and indeed is hard to define considering the given scatter in estimates. This reflects the shallow northeastward dip of this nappe, which indicates that samples in these sections originated in nearly identical structural levels.

## DISCUSSION

### Samples with anomalous peak-temperature values

Five samples (marked red in Table S1) yield anomalous  $T_p$  that do not fit the overall pattern. Four of these (samples 18, 105, 129 & 173) have values that are significantly lower, and one (sample 53) has significantly higher temperatures than nearby values despite the fact that all five samples come from the same lithology as their neighbours. There are two

possible explanations for this: either graphitization of organic matter in these samples depends on additional factors besides temperature (pressure, strain, etc. as discussed above) or, as is probably the case in sample 53, the sedimentary protoliths may have contained organic detritus eroded from areas that underwent pre-Alpine metamorphism at higher  $T_p$  (e.g. Dissel *et al.*, 1978; Itaya, 1981) than those reached during the Alpine events discussed here.

Another four specimens (samples 37, 48, 60 & 176) yield clear indications of dual-temperature signals for all calibrations (temperatures listed in Table S1 with an orange background), as will be discussed later. All these samples originate from similar lithologies within the KSZS and the same transparent minerals overlying the measured CM were used.

Close examination reveals local irregularities in the pattern of  $T_p$  in domain 3: in the Upper Muhr Valley (Figs 2 & 4),  $T_p$  values scatter widely in the Modeck- and Glockner nappe systems along the steep northern branch of the KSZS.

#### Comparison with peak temperatures from other petrological data

The calibrations of Beyssac *et al.* (2002b) and Aoya *et al.* (2010) yield  $T_p$  values that are closest to the temperatures obtained from peak-metamorphic mineral assemblages in the eastern Tauern Window (calibrations a and d in Table 1). This is best demonstrated in two areas:

In a first area along the southwestern margin of the ETD (i.e. parallel to the southern sinistral branch of the KSZS, Fig. 2a), the coexistence of garnet, biotite and chloritoid, as well as the location within the staurolite + biotite isograd (Droop, 1981, 1985), constrains  $T_p$  during the 'Tauernkristallisation' to 500–550 °C (Fig. 2a). This brackets the peak-temperature estimates obtained from the two aforementioned calibrations (a and d in Table 1) to 500 and 510 °C respectively. The other calibration methods (b and c in Table 1; Rahl *et al.*, 2005; Aoya *et al.*, 2010) yield 475 and 485 °C respectively. In a second area in the core of the Hochalm Dome, felsic gneiss contains garnet, green amphibole and biotite in the absence of evidence for partial melting. The temperature in this area therefore never exceeded 650 °C, the minimum temperature for the onset of melting of water-saturated granitic rock (e.g. Holtz *et al.*, 2001). This is corroborated by temperature estimates of  $630 \pm 40$  °C from phase equilibria (Droop, 1985). All RSCM calibrations yield  $T_p$  slightly below this value for the same locality (612, 640, 632 °C for calibrations a, c and d in Table 1), with the exception of the Rahl *et al.* (2005) calibration, which yields 680 °C (Appendix S1; Table S1). In general, all of the calibrations except that of Rahl *et al.* (2005) provide similar estimates of  $T_p$  for the range of ~350–620 °C. However, the difference in the peak-tempera-

ture estimates is certainly much less than the uncertainty of  $\pm 50$  °C (Appendix S1; Fig. S2) and demonstrates the excellent consistency of the empirical calibrations so far.

#### Multiple temperature signals in the same sample

Four samples (samples 37, 48, 60 & 176; Table S1) yield more than one temperature signal as determined from separate clusters of Raman spectra. All of these anomalous samples come from the KSZS in domain 3; in two of them (48, 60), the lower of the two peak-temperature estimates agrees with the estimates from the surrounding samples in the area. However, this is not the case for the other two samples (37, 176). Thus, shearing may well have had an effect on the ordering of CM (Bustin *et al.*, 1986; Suchy *et al.*, 1997; Ferreiro Máhlmann *et al.*, 2002; Nover *et al.*, 2005), but the inconsistency of the  $T_p$  values in relation to the surrounding estimates leaves much room for speculation on whether this ordering increased or decreased during shearing. Alternatively, the multiple temperature signal is a kinetic effect that led to the partial equilibration of CM ordering with the regional metamorphism ('Tauernkristallisation') and a later, short-lived heating or fluid pulse (or both) when Katschberg shearing juxtaposed warm ( $\geq 525$  °C) rock from the hot core of the ETD with the margins of the ETD. This is consistent with the observation of post-kinematic (cross-) white mica that overgrows the main mylonitic foliation of the KSZS (Scharf, 2013). A third possibility is that the separate Raman spectra within one sample result from mixing of detrital sediments with different thermal provinces (Dissel *et al.*, 1978). This only explains samples 48 and 60 with a second temperature signal higher than the ambient  $T_p$  of neighbouring samples. In light of this unresolved problem, none of the four samples with more than one temperature signal was used in drawing the peak-temperature contours.

#### Age of peak temperatures

The  $T_p$  values determined with RSCM can only be interpreted in a geodynamic context if the age of metamorphic events in the three fabric domains and in the adjacent Austroalpine units that border the Tauern Window is known. The main foliation sampled in fabric domain 1 is deformed by both the SEMP Fault and by the northern branch of the KSZS (Fig. 2b). These faults are interpreted to have initiated in Latest Oligocene to Early Miocene time, certainly no later than *c.* 21 Ma, which marks the onset of Adriatic indentation and rapid exhumation in the Tauern Window (Scharf *et al.*, 2013; Schmid *et al.*, 2013; their D5). The  $^{40}\text{Ar}/^{39}\text{Ar}$  white mica ages of Liu *et al.* (2001) for this fabric domain in the South Penninic Mafrei Zone range in age from *c.* 36.8 to 28 Ma (excluding one sample with an age of

*c.* 21.8 Ma) and are interpreted to date cooling beneath the closure temperature range of 410–350 °C (Liu *et al.*, 2001 after von Blanckenburg *et al.*, 1989; Dahl, 1996). Regional geological considerations constrain the onset of accretion in the Matrei Zone, originally located at the southern limit of Alpine Tethys, to have begun no later than 94–84 Ma (e.g. Cenomanian-Santonian flysch ages as discussed in Handy *et al.*, 2010, and many references therein). Thus, the available information indicates that the main deformation and peak of metamorphism in fabric domain 1 occurred during Late Cretaceous to Late Palaeogene time.

High-pressure metamorphism in fabric domain 2 is constrained to have occurred within the *c.* 45–38 Ma time interval based on  $^{40}\text{Ar}/^{39}\text{Ar}$  phengite ages that are interpreted as syn-eclogite facies formational ages (Ratschbacher *et al.*, 2004; Kurz *et al.*, 2008). Younger ages were obtained with the Rb/Sr on white mica system (*c.* 31.5 ± 0.7 Ma; Glodny *et al.*, 2005, 2008) and the Lu/Hf on garnet chronometry *c.* 32.75 ± 0.5 Ma (Nagel *et al.*, 2013) for this same event. However, in the overall regional context, such Early Oligocene ages are unlikely for the baric peak for two reasons: First, these young ages are inconsistent with the Eocene age of high-pressure metamorphism in along-strike equivalents of the Subpenninic nappes and the Glockner Nappe System in the Engadine Window and the Lepontine Dome (*c.* 42–40 Ma for the Glockner Nappe System equivalent in the Engadine Window, Wiederkehr *et al.*, 2009; *c.* 42–35 Ma for the Adula Nappe in the Lepontine Dome, Berger & Bousquet, 2008; Herwartz *et al.*, 2011). Second, such young ages for high-pressure metamorphism are incompatible with the contemporaneous emplacement of the nearby Periadriatic plutons, which intruded at moderate depths during continent–continent collision and after the early stages of continental subduction (e.g. Rosenberg, 2004). In any case, the main schistosity in domain 2 is overgrown by upper greenschist to amphibolite facies mineral assemblages of the Oligocene ‘Tauernkristallisation’ (see Provenance of the sample section) and is deformed by large Miocene post-nappe folds (e.g. Sonnblick Dome, Fig. 2a). The high-pressure part of the Glockner Nappe System attained peak conditions of 1.7 GPa and 570 °C (Dachs & Proyer, 2001). The high pressure is documented by pseudomorphs after lawsonite (e.g. Grossglockner area west of the Sonnblick Dome, Fig. 2a, Gleissner *et al.*, 2007). The  $T_p$  is roughly compatible with the 500–535 °C range obtained from RSCM, although only four RSCM samples were used for this estimate in the general sample area of Dachs & Proyer (2001).

The two main foliations in fabric domain 3 (see Fig. 2b) are related to different tectonic events (Scharf *et al.*, 2013): (i) the older foliation formed under amphibolite facies conditions and was associated with stacking of the Subpenninic nappes in the

Venediger Duplex. It is syn- to post-thrusting and exhumation of the overlying high-pressure units in fabric domain 2 (Schmid *et al.*, 2013; their D4), but pre-dates the ‘Tauernkristallisation’ and subsequent doming (Schmid *et al.*, 2013; their D5). This older foliation formed at *c.* 35–30 Ma, as discussed extensively in Schmid *et al.* (2013), their D4; and (ii) the younger greenschist facies mylonitic foliation of the KSZS that overprints the perimeter of the ETD is constrained to have formed at *c.* 23–16 Ma, as discussed in Scharf (2013) and Schmid *et al.* (2013); their D5). This second event coincided with the formation of the Hochalm- and Sonnblick domes (Fig. 2a).

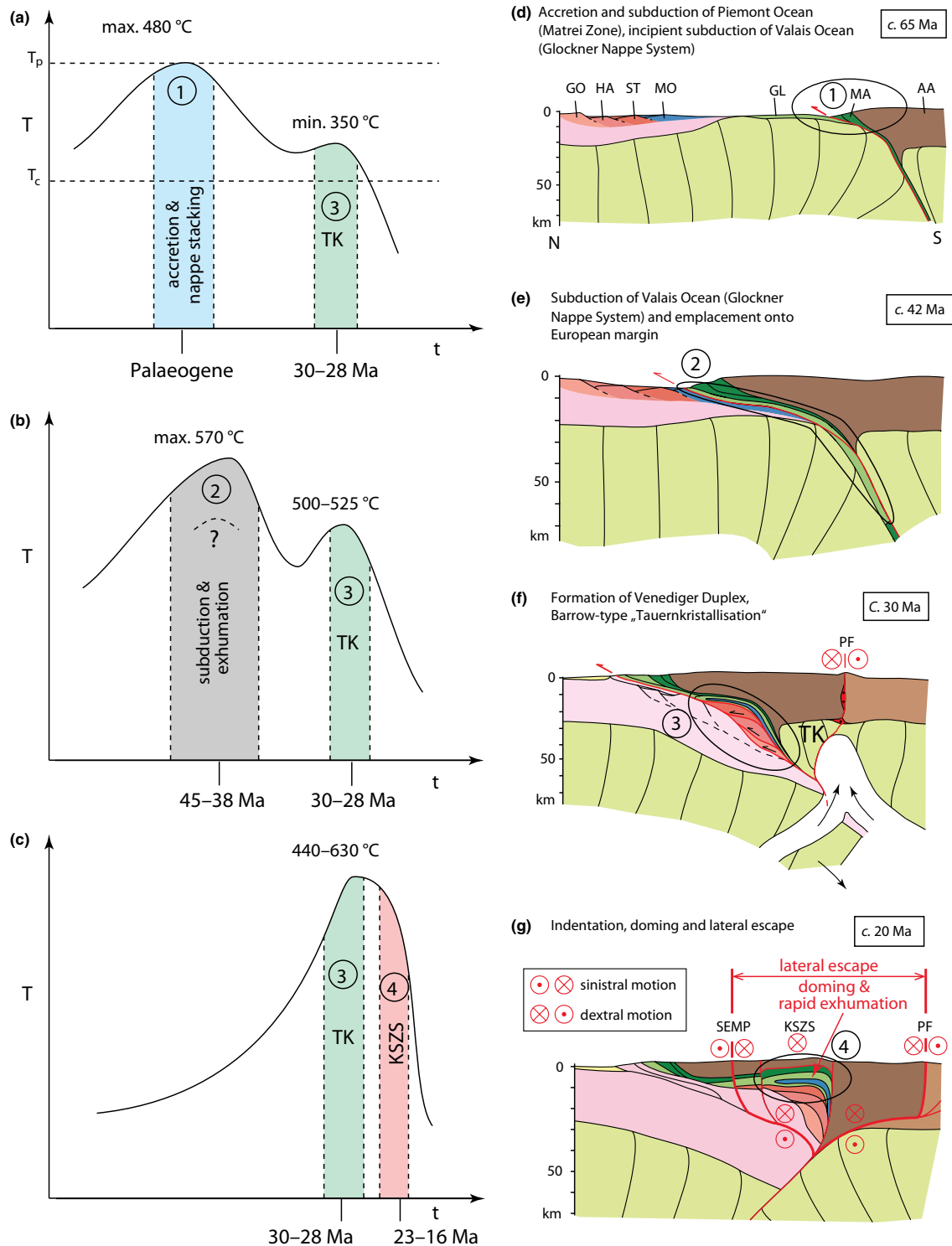
### The peak temperatures in a geodynamic context

Figure 6 is a first attempt to integrate the different  $T_p$  values obtained within the three fabric domains (Fig. 6a–c) in a tectonic context (Fig. 6d–g). Figure 6d–g shows the evolution in a north–south transect of the Tauern Window and builds on previous work (Kurz *et al.*, 2008; Scharf *et al.*, 2013; Schmid *et al.*, 2013). Each fabric domain is marked by a different thermal regime that corresponds to a distinct stage of convergence between Adria and Europe.

The maximum recorded temperature of ~480 °C in domain 1 is consistent with the greenschist facies metamorphism observed in this domain and is interpreted to have resulted from the accretion of oceanic crust of Alpine Tethys in the footwall of the Austroalpine nappes (samples 191 & 192 in Fig. 3; Table S1). The units in domain 1 thus represent the leading edge of the advancing Adriatic microplate in Palaeogene time (Fig. 5a,d). Similar peak conditions have been documented from the basal units of exhumed accretionary wedges in other localities (e.g. Taiwan, Suppe, 1984). The lack of any discernable jump in  $T_p$  across the thrust contact between the Glockner Nappe System and the Matrei Zone (Fig. 5a) indicates that the thermal peak in domain 1 was attained only after these two units, which derive from different parts of Alpine Tethys, were tectonically juxtaposed, i.e. after *c.* 65 Ma, but before *c.* 42 Ma (Fig. 6d,e).

The metamorphism in domain 1 is probably Late Eocene or older according to available  $^{40}\text{Ar}/^{39}\text{Ar}$  white mica ages of Liu *et al.* (2001). These ages indicate cooling of the Penninic nappes at the northeastern margin of the Tauern Window to below 410–350 °C in Late Oligocene time (Liu *et al.*, 2001), with ages progressively older (Eocene) towards the Lower Austroalpine nappes in the hangingwall of the KSZS. Thus, metamorphism in the Penninic nappes certainly pre-dates the Oligocene ‘Tauernkristallisation’.

The post-peak thermal evolution of domain 1 is poorly constrained, but thermochronometric age studies so far indicate that the Matrei Zone as well as parts of the Glockner Nappe System that were unaffected by high-pressure metamorphism experi-



**Fig. 6.** Schematic peak temperature *v.* time curves (a–c) for the three fabric domains and their corresponding tectonic stages (d–g) as discussed in the text. Numbers 1–4 in (a–c) refer to the tectonic stages in (d–g). AA, Austroalpine nappes; GL, Glockner Nappe System; GO, Göss Nappe; HA, Hochalm Nappe; KSZS, Katschberg Shear Zone System; MA, Matrei Zone; MO, Modereck Nappe System; PF, Periadriatic Fault; SEMP, Salzach-Ennstal-Mariazell-Puchberg Fault; ST, Storz Nappe; TK, ‘Tauernkristallisation’. Legend as in Figs 1 & 2;  $T_c$ , closure temperature of the  $^{40}\text{Ar}/^{39}\text{Ar}$  system on white mica;  $T_p$ , peak temperature obtained in this study. Dashed curved line and question mark in (b) indicates that it is not known whether the peak-temperature conditions were derived during Eocene subduction and exhumation or during Late Oligocene Barrovian-type overprinting (‘Tauernkristallisation’).

enced the Late Oligocene 'Tauernkristallisation' (labelled TK in Fig. 6). Two  $^{40}\text{Ar}/^{39}\text{Ar}$  white mica cooling ages of Liu *et al.* (2001) (their samples YL10, YL12) show that these units cooled to below 410–350 °C some *c.* 28 Ma ago. Thus, temperatures during the 'Tauernkristallisation' must have exceeded 410–350 °C, but not the previous peak of 480 °C (Fig. 6a). There is currently no sensible explanation of the single Miocene  $^{40}\text{Ar}/^{39}\text{Ar}$  white mica age in the part of the Matri Zone in the hangingwall of the northern corner of the KSZS (*c.* 21.7 Ma, Liu *et al.*, 2001; their sample YL40). This area coincides with a local 'island' of higher  $T_p$  (475–500 °C intervals in Figs 4 & 5d) that is interpreted as a thermal relict of domain 1.

Samples from domain 2 in the Glockner Nappe System yield  $T_p$  of 500–535 °C. None of them preserve high-pressure mineral assemblages, although eclogite facies minerals occur in a surrounding imbricate zone that comprises slices of both oceanic (Glockner Nappe System) and European continental margin (Modereck Nappe System, Pestal *et al.*, 2009; sample 200, Table S1). These  $T_p$  prevailed during both the eclogite facies event (570 °C; Dachs & Proyer, 2001) and the overprinting 'Tauernkristallisation' (no cooling ages obtained in this area, but Dachs, 1990; determined 525 °C in the eclogite zone, Fig. 1). Unfortunately, it is not known which of these two events was recorded by the CM Raman spectra in this domain (Fig. 6b).

Our data support the notion that all rocks of fabric domain 3 (Fig. 2b) are affected by Oligocene amphibolite- to greenschist facies Barrovian-type metamorphism ('Tauernkristallisation'), which is attributed to thickening of the European crust (Venediger Duplex formation, Fig. 6f).  $T_p$  values range from 440 °C in the Glockner Nappe System to 612 °C in the cover rocks of the Göss Nappe. The perimeter of the ETD has very steep field gradients in  $T_p$ , especially in the footwall of the KNF where the maximum gradient (up to 70 °C km<sup>-1</sup>) coincides with the site of maximum tectonic thinning of the Subpenninic- and Penninic units (Scharf *et al.*, 2013). The original (pre-Katschberg) peak gradient was only ~13 °C km<sup>-1</sup> as obtained by dividing the difference in  $T_p$  between the bottom (612 °C) and top (440 °C) of the nappe pile by the estimated 13.5 km of throw along the KNF (Scharf *et al.*, 2013).

## CONCLUSIONS

The RSCM method, combined with structural and petrological field data, yields a picture of the peak-temperature patterns associated with different stages of orogenesis in the eastern Tauern Window. This area has many features in common with the Lepontine Dome of the Central Alps, which exposes similar tectonic units with a similar thermal evolution (e.g. Wiederkehr *et al.*, 2011). The peak-temperature pat-

terns differ in three distinct structural and fabric domains of the Tauern Window: (i) Penninic units derived from the Alpine Tethys (Matri Zone and Glockner Nappes System) attained a maximum peak temperature ( $T_p$ ) of ~480 °C under upper greenschist facies conditions during and after Late Cretaceous to Palaeogene nappe stacking in an accretionary wedge at the leading edge of the advancing Adriatic micro-plate; (ii) imbricated and folded oceanic and distal continental European units experienced  $T_p$  of ~500–535 °C. These temperatures were attained either during Palaeogene burial and exhumation along a narrow subduction/exhumation channel in the central eastern part of the Tauern Window, or during Barrovian-type thermal overprinting at the margins of the Eastern Tauern Subdome; and (iii) a duplex of basement slices derived from the European margin experienced  $T_p$  immediately after D4 nappe stacking, i.e. in the Early Oligocene. However, these same peak-temperature contours of this pattern acquired their current concentric form during Miocene post-nappe doming and extensional shearing along the KSZS. The  $T_p$  values in the largest dome (Hochalm Dome) range from 612 °C in its core to 440 °C at its rim. The steepest gradient in  $T_p$  (up to 70 °C km<sup>-1</sup>) occurs perpendicular to the eastern margin of this dome, where mylonitic shearing of the KNF significantly thinned the Subpenninic- and Penninic nappe pile, including an older  $T_p$  distribution.

The large number (200) of samples analysed in this study provides an excellent basis for comparing  $T_p$  derived from RSCM with those from peak-metamorphic mineral assemblages. It was found that the Raman spectra calibrations of Beyssac *et al.* (2002b) and Aoya *et al.* (2010) (calibration d in Table 1) are in closest agreement with the petrology, especially at higher (>500 °C)  $T_p$ . Interestingly, all calibrations yield very similar patterns of  $T_p$  values within each fabric domain and, even more strikingly, the differences in these temperature estimates are less than the ±50 °C absolute error of the calibrations (Beyssac *et al.*, 2002b). This is testimony to the robustness of the RSCM method, even when applied to areas with a polyphase metamorphic history.

## ACKNOWLEDGEMENTS

We are indebted to many colleagues for discussions, especially A. Bertrand, S. Favaro, K. Hammer-schmidt, S. Schneider and C.L. Rosenberg, all from the Freie Universität Berlin, as well as R. Schuster and G. Pestal from the Austrian Geological Survey in Vienna, and B. Fügenschuh from the Universität Innsbruck. Special thanks go to R. Oberhänsli who kindly supported our work at the Universität Potsdam. A. Giribaldi and S. Wollnik (both Freie Universität Berlin) are thanked for preparing thin-sections. M. Grundmann is particularly thanked for drafting the figures. Finally, we acknowledge the sup-

port of the National Park Services Hohe Tauern, in particular of K. Aichhorn and the staff of the Bios Zentrum in Mallnitz. Our work was largely financed by the German Science Foundation (DFG-project Ha 2403/10). S.M. Schmid acknowledges the Alexander-von-Humboldt Foundation for support of his collaborative research in Berlin from 2008 to 2010. For a very critical and constructive journal reviewing, the reviewer (M. Wiederkehr and an anonymous reviewer) and the editor in chief (D. Robinson) are explicitly thanked.

## REFERENCES

- Aoya, M., Kouketsu, Y., Endo, S. *et al.*, 2010. Extending the applicability of the Raman carbonaceous-material geothermometer using data from contact metamorphic rocks. *Journal of Metamorphic Geology*, **28**, 895–914. doi: 10.1111/j.1525-1314.2010.00896.x.
- Becker, B., 1993. The structural evolution of the Radstadt thrust system, Eastern Alps, Austria – Kinematics, thrust geometries, strain analysis. *Tübinger Geowissenschaftliche Arbeiten*, **92(A)**, 1–83.
- Berger, A. & Bousquet, R., 2008. Subduction-related metamorphism in the Alps: review of isotopic ages based on petrology and their geodynamic consequences. In: *Tectonic Aspects of the Alpine-Dinaride-Carpathian System* (eds Siegmund, S., Fügenschuh, S.B. & Froitzheim, N.), pp. 117–144. Geological Society, London, Special Publications, 298.
- Beysac, O., Rouzaud, J.N., Goffé, B., Brunet, F. & Chopin, C., 2002a. Graphitization in a high-pressure, low-temperature metamorphic gradient: a Raman microspectroscopy and HRTEM study. *Contributions to Mineralogy and Petrology*, **143**, 19–31.
- Beysac, O., Goffé, B., Chopin, C. & Rouzaud, J.N., 2002b. Raman spectra of carbonaceous material in metasediments: a new geothermometer. *Journal of Metamorphic Geology*, **20**, 859–871.
- Beysac, O., Brunet, F., Petit, J.P., Goffé, B. & Rouzaud, J.N., 2003a. Experimental study of the microtextural and structural transformations of carbonaceous material under pressure and temperature. *European Journal of Mineralogy*, **15**, 937–951.
- Beysac, O., Goffé, B., Petit, J.P., Froigneux, E., Moreau, M. & Rouzaud, J.N., 2003b. On the characterization of disordered and heterogeneous carbonaceous materials by Raman spectroscopy. *Spectrochimica Acta Part A – Molecular and Biomolecular Spectroscopy*, **59**, 2267–2276.
- Beysac, O., Bollinger, L., Avouac, J.P. & Goffé, B., 2004. Thermal metamorphism in the lesser Himalaya of Nepal determined from Raman spectroscopy of carbonaceous material. *Earth and Planetary Science Letters*, **225**, 233–241.
- von Blanckenburg, F., Villa, I.M., Baur, H., Morteani, G. & Steiger, R.H., 1989. Time calibration of a PT-path from the Western Tauern Window, Eastern Alps: the problem of closure temperatures. *Contributions Mineralogy and Petrology*, **101**, 1–11.
- Bonijoly, M., Oberlin, M. & Oberlin, A., 1982. A possible mechanism for natural graphite formation. *International Journal of Coal Geology*, **1**, 238–312.
- Buseck, P.R. & Bo-Jun, H., 1985. Conversion of carbonaceous material to graphite during metamorphism. *Geochimica et Cosmochimica Acta*, **49**, 2003–2016.
- Bustin, R.M., Ross, J.V. & Moffat, I., 1986. Vitrinite anisotropy under differential stress and high confining pressure and temperature: preliminary observations. *International Journal of Coal Geology*, **6**, 343–351.
- Bustin, R.M., Ross, J.V. & Rouzaud, J.N., 1995. Mechanism of graphite formation from kerogen: experimental evidence. *International Journal of Coal Geology*, **28**, 1–36.
- Cliff, R.A., Droop, G.T.R. & Rex, D.C., 1985. Alpine metamorphism in the south-east Tauern Window, Austria: 2. Rates of heating, cooling and uplift. *Journal of Metamorphic Geology*, **3**, 403–415.
- Dachs, E., 1986. High-pressure mineral assemblages and their breakdown products in metasediments south of the Grossvenediger, Tauern Window, Austria. *Schweizerische Mineralogische und Petrographische Mitteilungen*, **66**, 145–161.
- Dachs, E., 1990. Geothermobarometry in metasediments of the southern Grossvenediger area (Tauern Window, Austria). *Journal of Metamorphic Geology*, **8**, 217–230.
- Dachs, E. & Proyer, A., 2001. Relics of high-pressure metamorphism from the Grossglockner region, Hohe Tauern, Austria, paragenetic evolution and PT-paths of retrogressed eclogites. *European Journal of Mineralogy*, **13**, 67–86.
- Dahl, P.S., 1996. The crystal-chemical basis for Ar retention in micas: inferences from interlayer partitioning and implications for geochronology. *Contributions to Mineralogy and Petrology*, **123**, 22–39.
- Dissel, C.F.K., Brothers, R.N. & Black, P.M., 1978. Coalification and graphitization in high-pressure schists in New Caledonia. *Contributions to Mineralogy and Petrology*, **68**, 63–78.
- Droop, G.T.R., 1981. Alpine metamorphism of polydeformed schists in the south-east Tauern Window, Austria. *Schweizerische Mineralogische und Petrographische Mitteilungen*, **61**, 237–273.
- Droop, G.T.R., 1985. Alpine metamorphism in the south-east Tauern Window, Austria: 1. P-T variations in space and time. *Journal of Metamorphic Geology*, **3**, 371–402.
- Exner, C., 1939. Das Ostende der Hohen Tauern zwischen Mur- und Maltatal (I. Teil). *Jahrbuch Zweigstelle Wien Reichsstelle Bodenforschung (Jahrbuch Geologischen Bundesanstalt)*, **89**, 285–314.
- Exner, C., 1971. Aufnahmen 1970 auf Blatt Muhr (156) und Vergleichsbegehungen auf Blatt Spittal a. d. Drau (182). *Verhandlungen der Geologischen Bundesanstalt Wien*, **1971/4**, 28–30.
- Exner, C., 1980. Geologie der Hohen Tauern bei Gmünd in Kärnten. *Jahrbuch der Geologischen Bundesanstalt*, **123**, 343–410.
- Ferreiro Mählmann, R., Petrova, T.V., Pironon, J. *et al.*, 2002. Transmission electron microscopy study of carbonaceous material in a metamorphic profile from diagenesis to amphibolite facies (Bündnerschiefer, Eastern Switzerland). *Schweizerische Mineralogische und Petrographische Mitteilungen*, **82**, 253–272.
- Frasl, G. & Frank, W., 1966. Einführung in die Geologie und Petrographie des Penninikums im Tauernfenster mit besonderer Berücksichtigung des Mittelabschnittes im Oberpinzgau, Land Salzburg. *Der Aufschluß, Sonderheft*, **15**, 30–58.
- French, B.M., 1964. Graphitization of organic material in a progressively metamorphosed Precambrian iron formation. *Science*, **146**, 917–918.
- Frisch, W., 1979. Tectonic progradation and plate tectonic evolution of the Alps. *Tectonophysics*, **60**, 121–139.
- Frost, E., Dolan, J., Ratschbacher, L., Hacker, B. & Seward, G., 2011. Direct observation of fault zone structure at the brittle-ductile transition along the Salzach-Ennstal-Mariazell-Puchberg fault system, Austrian Alps. *Journal of Geophysical Research*, **116**, B02411. doi: 10.1029/2010JB007719.
- Genser, J. & Neubauer, F., 1989. Low angle normal faults at the eastern margin of the Tauern Window (Eastern Alps). *Mitteilungen der österreichischen Geologischen Gesellschaft*, **81**, 233–243.
- Gleissner, P., Glodny, J. & Franz, G., 2007. Rb-Sr isotopic dating of pseudomorphs after lawsonite in metabasalts

- from the Glockner nappe, Tauern Window, Eastern Alps. *European Journal of Mineralogy*, **19**, 723–734.
- Glodny, J., Ring, U., Kühn, A., Gleissner, P. & Franz, G., 2005. Crystallization and very rapid exhumation of the youngest Alpine eclogites (Tauern Window, Eastern Alps) from Rb/Sr mineral assemblage analysis. *Contributions to Mineralogy and Petrology*, **149**, 699–712.
- Glodny, J., Ring, U. & Kühn, A., 2008. Coeval high-pressure metamorphism, thrusting, strike-slip, and extensional shearing in the Tauern Window, Eastern Alps. *Tectonics*, **27**, TC4004. doi: 10.1029/2007TC002193.
- Grew, E.S., 1974. Carbonaceous material in some metamorphic rocks of New England and other areas. *Journal of Geology*, **82**, 50–73.
- Guedes, A., Noronha, F. & Prieto, A.C., 2005. Characterization of dispersed organic matter from lower Palaeozoic metasedimentary rocks by organic petrography, X-ray diffraction and micro-Raman spectroscopy analyses. *International Journal of Coal Geology*, **62**, 237–249.
- Haas, J., Kovacs, S., Krystin, L. & Lein, R., 1995. Significance of Late Permian-Triassic facies zones in terrain reconstructions in the Alpine-North Pannonic domain. *Tectonophysics*, **242**, 19–40.
- Handy, M.R., Schmid, S.M., Bousquet, R., Kissling, E. & Bernoulli, D., 2010. Reconciling plate tectonic reconstructions of Alpine Tethys with the geological–geophysical record of spreading and subduction in the Alps. *Earth-Science Reviews*, **102**, 121–158.
- Hejl, E., 1984. Geochronologische und Petrologische Beiträge zur Gesteinsmetamorphose der Schladminger Tauern. *Mitteilungen der Gesellschaft der Geologie- und Bergbaustudenten in Österreich*, **30/31**, 289–312.
- Herwartz, D., Nagel, T.J., Münker, C., Scherer, E.E. & Froitzheim, N., 2011. Tracing two orogenic cycles in one eclogite sample by Lu-Hf garnet chronometry. *Nature Geoscience*, **4**, 178–183.
- Hoinkes, G., Koller, F., Rantitsch, G. *et al.*, 1999. Alpine metamorphism of the Eastern Alps. *Schweizerische Mineralogische und Petrographische Mitteilungen*, **79**, 155–181.
- Holtz, F., Johannes, W., Tamic, N. & Behrens, H., 2001. Maximum and minimum water contents of granitic melts generated in the crust: a reevaluation and implications. *Lithos*, **56**, 1–14.
- Inger, S. & Cliff, R.A., 1994. Timing of metamorphism in the Tauern Window, Eastern Alps: Rb-Sr ages and fabric formation. *Journal of metamorphic Geology*, **12**, 695–707.
- Itaya, T., 1981. Carbonaceous material in pelitic schists of the Sanbagawa metamorphic belt in central – Shikoku, Japan. *Lithos*, **14**, 215–224.
- Kebede, T., Klötzli, U.S. & Pestal, G., 2003. Single zircon U-Pb geochronology of pre-variscan and variscan basement units of the central Tauern window, Eastern Alps (Austria). *Mitteilungen der Österreichischen Mineralogischen Gesellschaft*, **148**, 182–184.
- Kribek, B., Hrabal, J., Landais, P. & Hladikova, J., 1994. The association of poorly ordered graphite, coke and bitumens in greenschist facies rocks of the Ponikla Group, Lügicum, Czech Republic: the results of graphitization on various types of carbonaceous matter. *Journal of Metamorphic Geology*, **12**, 493–503.
- Kurz, W., Handler, R. & Bertoldi, C., 2008. Tracing the exhumation of the eclogite zone (Tauern Window, Eastern Alps) by  $^{40}\text{Ar}/^{39}\text{Ar}$  dating of white mica in eclogites. *Swiss Journal of Geoscience*, **101**, 191–206. doi: 10.1007/s00015-008-1281-1.
- Lahfid, A., Beyssac, O., Deville, E., Negro, F., Chopin, C. & Goffé, B., 2010. Evolution of Raman spectrum of carbonaceous material in low-grade metasediments of the Glarus Alps (Switzerland). *Terra Nova*, **22**, 354–360. doi: 10.1111/j.1365-3121.2010.00956.x.
- Landis, C.A., 1971. Graphitization of dispersed carbonaceous material in metamorphic rocks. *Contributions to Mineralogy and Petrology*, **30**, 34–45.
- Large, D.J., Christy, A.G. & Fallick, A.E., 1994. Poorly crystalline carbonaceous matter in high grade metasediments: implications for graphitization and metamorphic fluid composition. *Contributions to Mineralogy and Petrology*, **116**, 108–116.
- Lemoine, M., Bailot, G. & Tricart, P., 1987. Ultramafic and gabbroic ocean floor of the Ligurian Tethys (Alps, Corsica, Apennines): in search of a genetic model. *Geology*, **15**, 622–625.
- Lerchbauer, L., 2008. Petrographical, geochemical and geochronological investigations on the Variscan basement in the Kleinellental/Hohe Tauern (eastern Tauern Window, Austria). Diploma-thesis, Universität Wien, Vienna, 117 S.
- Liu, Y., Genser, J., Handler, R., Friedl, G. & Neubauer, F., 2001.  $^{40}\text{Ar}/^{39}\text{Ar}$  muscovite ages from the Penninic-Austroalpine plate boundary, Eastern Alps. *Tectonics*, **20**, 526–547.
- Nagel, T.J., Herwartz, D., Rexroth, S., Münker, C., Froitzheim, N. & Kurz, W., 2013. Lu-Hf dating, petrography, and tectonic implications of the youngest Alpine eclogites (Tauern Window, Austria). *Lithos*, **170–171**, 179–190.
- Nemanich, R.J. & Solin, S.A., 1979. First- and second-order Raman scattering from finite-size crystals of graphite. *Physical Review*, **B 20**, 392–401.
- Nover, G., Stoll, J.B. & von der Gönna, J., 2005. Promotion of graphite formation by tectonic stress – a laboratory experiment. *Geophysical Journal International*, **160**, 1059–1067.
- Oberhänsli, R., Bousquet, R., Engi, M. *et al.*, 2004. Metamorphic structure of the Alps. 1:1'000'000. Commission for the Geological Map of the World, Paris.
- Okuyama-Kusunose, Y. & Itaya, T., 1987. Metamorphism of carbonaceous material in the Tono contact aureole, Kitakami Mountains, Japan. *Journal of Metamorphic Geology*, **5**, 121–139.
- Pasteris, J.F., 1989. In situ analysis in geological thin-sections by laser Raman microprobe microspectroscopy: a cautionary note. *Applied Spectroscopy*, **43**, 567–570.
- Pasteris, J.D. & Wopenka, B., 1991. Raman-spectra of graphite as indicators of degree of metamorphism. *Canadian Mineralogist*, **29**, 1–9.
- Pestal, G. & Hejl, E., 2005. *Geologische Karte von Salzburg 1:200.000*. Geologische Bundesanstalt, Wien.
- Pestal, G. & Hellerschmidt-Alber, J., 2011. Bericht 2009 und 2010 über geologische Aufnahmen auf Blatt 154 Rauris. *Jahrbuch der Geologischen Bundesanstalt*, **151**, 142–147.
- Pestal, G., Hejl, E., Braunstingl, R. & Schuster, R., 2009. *Erläuterungen zur geologischen Karte von Salzburg 1:200.000*. Geologische Bundesanstalt, Wien.
- Quinn, A.W. & Glass, H.D., 1958. Rank of coal and metamorphic grade rocks of Narragansett basin of Rhode Island. *Economic Geology*, **53**, 563–576.
- Rahl, J.M., Anderson, K.M., Brandon, M.T. & Fassoulas, C., 2005. Raman spectroscopic carbonaceous material thermometry of low-grade metamorphic rocks: calibration and application to tectonic exhumation in Crete, Greece. *Earth and Planetary Science Letters*, **240**, 339–354.
- Ratschbacher, L., Frisch, W., Linzer, H.-G. & Merle, O., 1991. Lateral extrusion in the Eastern Alps, part 2: structural analysis. *Tectonics*, **10**, 257–271.
- Ratschbacher, L., Dingeldey, C., Miller, C., Hacker, B.R. & McWilliams, M.O., 2004. Formation, subduction, and exhumation of Penninic oceanic crust in the Eastern Alps: time constraints from  $^{40}\text{Ar}/^{39}\text{Ar}$  geochronology. *Tectonophysics*, **394**, 155–170.
- Rosenberg, C.L., 2004. Shear zones and magma ascent: a model based on a review of the tertiary magmatism in the Alps. *Tectonics*, **23**. doi: 10.1029/2003TC001526.
- Sander, B., 1911. Geologische Studien am Westende der hohen Tauern. *Bericht – Denkschrift der kaiserlichen Akademie der Wissenschaften Wien*, **83**, 257–319.
- Scharf, A., 2013. Lateral Extrusion and Exhumation of Orogenic Crust during Indentation by Rigid Adriatic Continental Lithosphere – Tectonic Evolution of the Eastern Tauern

- Window (Eastern Alps, Austria). Dissertation, Freie Universität Berlin, Berlin.
- Scharf, A., Handy, M.R., Favaro, S., Schmid, S.M. & Bertrand, A., 2013. Modes of orogen-parallel stretching and extensional exhumation in response to microplate indentation and roll-back subduction (Tauern Window, Eastern Alps). *International Journal of Earth Sciences*. doi: 10.1007/s00531-013-0894-4.
- Schmid, S.M., Fügenschuh, B., Kissling, E. & Schuster, R., 2004. Tectonic map and overall architecture of the Alpine orogen. *Eclogae geologicae Helveticae*, **97**, 93–117.
- Schmid, S.M., Scharf, A., Handy, M.R. & Rosenberg, C.L., 2013. The Tauern Window (Eastern Alps, Austria) – a new tectonic map, cross-sections and tectonometamorphic synthesis. *Swiss Journal of Geosciences*, **106**, 1–32.
- Schönlaub, H.P., Exner, C. & Nowotny, A., 1976. Das Altpaläozoikum des Katschberges und seiner Umgebung (Österreich). *Verhandlungen der Geologischen Bundesanstalt*, 115–146.
- Schramm, J.M., 1980. Bemerkungen zum Metamorphosegeschehen in klastischen Sedimentgesteinen im Salzburger Abschnitt der Grauwackenzone und der Nördlichen Kalkalpen. *Mitteilungen der Österreichischen Geologischen Gesellschaft*, **71/72**, 379–384.
- Schuster, R., Koller, F., Hoek, V., Hoinkes, G. & Bousquet, R., 2004. Explanatory notes to the map metamorphic structure of the Alps. *Mitteilungen der Österreichischen Mineralogischen Gesellschaft*, **149**, 175–199.
- Schuster, R., Pestal, G. & Reitner, J.M., 2006. Erläuterungen zu Blatt 182 Spittal an der Drau, Geologische Karte der Republik Österreich 1:50.000, Wien 2006.
- Selverstone, J., Spear, F.S., Franz, G. & Morteau, G., 1984. High-pressure metamorphism in the SW Tauern Window, Austria: P-T paths from Hornblende-Kyanite-Stauroilite Schists. *Journal of Petrology*, **25**, 501–531.
- Slapansky, P. & Frank, W., 1987. Structural evolution and geochronology of the northern margin of the Austroalpine in the northwestern Schladming Crystalline. In: *Geodynamics of the Eastern Alps* (eds Flügel, H.W. & P. Faupl, P.), pp. 244–262. Deuticke, Vienna.
- Stampfli, G., Mosar, J., Favre, P., Pilleveit, A. & Vannay, J.-C., 2001. Permo-Mesozoic evolution of the western Tethys realm: the Neo-Tethys East Mediterranean Basin connection. In: *Peri-Tethys Memoir 6: Peri-Tethyan Rift/Wrench Basins and Passive Margins* (eds Ziegler, P.A. et al.), pp. 51–108. Mémoires du Muséum National d'histoire Naturelle, Paris, 186.
- Suchy, V., Frey, M. & Wolf, M., 1997. Vitrinite reflectance and shear-induced graphitization in orogenic belts: a case study from the Kandersteg area, Helvetic Alps, Switzerland. *International Journal of Coal Geology*, **34**, 1–20.
- Suppe, J., 1984. Kinematics of arc-continent collision, flipping of subduction, and back-arc spreading near Taiwan. *Memoir of the Geological Society of China*, **6**, 21–33.
- Teichmüller, M., 1987. Organic material and very low-grade metamorphism. In: *Low Temperature Metamorphism* (ed. Frey, M.), pp. 114–161. Blackie, Glasgow and London.
- Thöni, M., 1999. A review of geochronological data from the Eastern Alps. *Schweizerische Mineralogische und Petrographische Mitteilungen*, **79/1**, 209–230.
- Thöni, M., 2006. Dating eclogite-facies metamorphism in the Eastern Alps – approaches, results, interpretations: a review. *Mineralogy and Petrology*, **88**, 123–148.
- Tricart, P., 1984. From passive margin to continental collision: a tectonic scenario for the Western Alps. *American Journal of Sciences*, **284**, 97–120.
- Trümpy, R., 1960. Paleotectonic evolution of the Central and Western Alps. *Bulletin Geological Society of America*, **71**, 843–908.
- Urbanek, C., Frank, W., Grasmann, B. & Decker, K., 2002. Eoalpine versus Tertiary deformation: Dating of heterogeneously partitioned strain (Tauern Window, Austria). *Pan-geo Austria: Erdwissenschaften in Österreich 28.-30.6.2002* (Program and abstract), Institute for geology and paleontology University of Salzburg.
- Veselá, P., Lammerer, B., Wetzel, A., Söllner, F. & Gerdes, A., 2008. Post-Variscan to Early Alpine sedimentary basins in the Tauern Window (Eastern Alps). In: *Tectonic Aspects of the Alpine-Dinaride-Carpathian System* (eds Siegesmund, S., Fügenschuh, B. & Froitzheim, N.), pp. 83–100. Geological Society, London, Special Publications, 298.
- Veselá, P., Söllner, F., Finger, F. & Gerdes, A., 2011. Magmato-sedimentary Carboniferous to Jurassic evolution of the western Tauern window, Eastern Alps (constraints from U-Pb zircon dating and geochemistry). *International Journal of Earth Sciences*, **100**, 993–1027.
- Wada, H., Tomita, T., Matsuura, K., Iuchi, K., Ito, M. & Morikyo, T., 1994. Graphitization of carbonaceous matter during metamorphism with references to carbonate and polytic rocks of contact and regional metamorphism, Japan. *Contributions to Mineralogy and Petrology*, **118**, 217–228.
- Wiederkehr, M., Sudo, M., Bousquet, R., Berger, A. & Schmid, S.M., 2009. Alpine orogenic evolution from subduction to collisional thermal overprint: the  $^{40}\text{Ar}/^{39}\text{Ar}$  age constraints from the Valaisan Ocean, Central Alps. *Tectonics*, **28**, 1–28TC6009. doi: 10.1029/2009TC002496.
- Wiederkehr, M., Bousquet, R., Ziemann, M.A., Berger, A. & Schmid, S.M., 2011. 3-D assessment of peak-metamorphic conditions by Raman spectroscopy of carbonaceous material: an example from the margin of the Lepontine dome (Swiss Central Alps). *International Journal of Earth Sciences*, **100**, 1029–1063.
- Wopenka, B. & Pasteris, J.D., 1993. Structural characterization of kerogens to granulite-facies graphite – applicability of Raman microprobe spectroscopy. *American Mineralogist*, **78**, 533–447.
- Yui, T.F., Huang, E. & Xu, J., 1996. Raman spectrum of carbonaceous material: a possible metamorphic grade indicator for low-grade metamorphic rocks. *Journal of Metamorphic Geology*, **14**, 115–124.
- Zimmermann, R., Hammerschmidt, K. & Franz, G., 1994. Eocene high pressure metamorphism in the Penninic units of the Tauern Window (Eastern Alps) – evidence from  $\text{Ar}^{40}$ – $\text{Ar}^{39}$  dating and petrological investigations. *Contributions to Mineralogy and Petrology*, **117**, 175–186.

## SUPPORTING INFORMATION

Additional Supporting Information may be found in the online version of this article at the publisher's web site:

**Appendix S1:** Raman spectra of carbonaceous material.

**Figure S1:** Typical first-order Raman spectra of CM showing increasing ordering with increasing peak temperature from bottom to top.

**Figure S2:** Peak-temperature comparison plots with calibration a on the vertical axis v. calibrations b, c and d on the horizontal axis.

**Figure S3:** Peak-temperature contours in fabric domains 1 and 3 (Fig. 2b) are based on the calibrations of (a) Rahl et al. (2005); (b) Aoya et al. (2010, calibration c in Table 1); and (c) Aoya et al. (2010, calibration d in Table 1).

**Table S1:** RSCM samples analysed in this study, as discussed in the Lithologies section and shown in Fig. 3.

Received 18 December 2012; revision accepted 20 July 2013.